Design of pH-responsive antimicrobial peptide melittin analog-camptothecin conjugates for tumor therapy

Sujie Huang [a,b,1], Yuxuan Gao [a,b,1], Ling Ma [a,b], Bo Jia [b], Wenhao Zhao [d], Yufan Yao [b], Wenyuan Li [b], Tongyi Lin [d], Rui Wang [b], Jingjing Song [a,b,], Wei Zhang [b,c,*]*

[a] *Institute of Pharmacology, School of Basic Medical Sciences, Lanzhou University, Lanzhou 730000, China*
[b] *Key Laboratory of Preclinical Study for New Drugs of Gansu Province, School of Basic Medical Sciences & Research Unit of Peptide Science, Chinese Academy of Medical Sciences, Lanzhou University, Lanzhou 730000, China*
[c] *State Key Laboratory of Veterinary Etiological Biology, College of Veterinary Medicine, Lanzhou University, Lanzhou 730000, China*
[d] *Lanzhou University Second Hospital, Lanzhou University, Lanzhou 730000, China*

ARTICLE INFO

ABSTRACT

Melittin, a classical antimicrobial peptide, is a highly potent antitumor agent. However, its significant toxicity seriously hampers its application in tumor therapy. In this study, we developed novel melittin analogs with pH-responsive, cell-penetrating and membrane-lytic activities by replacing arginine and lysine with histidine. After conjugation with camptothecin (CPT), CPT-AAM-1 and CPT-AAM-2 were capable of killing tumor cells by releasing CPT at low concentrations and disrupting cell membranes at high concentrations under acidic conditions. Notably, we found that the C-terminus of the melittin analogs was more suitable for drug conjugation than the N-terminus. CPT-AAM-1 significantly suppressed melanoma growth *in vivo* with relatively low toxicity. Collectively, the present study demonstrates that the development of antitumor drugs based on pH-responsive antimicrobial peptide-drug conjugates is a promising strategy.

1. Introduction

Melanoma is a heterogeneous and aggressive kind of skin neoplasm. Despite recent advances in tumor therapy, melanoma treatment faces enormous challenges. Melanoma is notorious for its resistance to conventional chemotherapy; however, it responds well to intratumoral immunotherapy [1]. The injection of an oncolytic virus has been proven to be an effective approach for treating melanoma. Oncolytic viruses mediate antitumor activity by directly lysing tumor cells and subsequently inducing antitumor immune responses [1–4]. Similar to oncolytic viruses, antimicrobial peptides (AMPs) with membrane-lytic activity are promising antitumor agents that target tumor heterogeneity [4]. Currently, some AMPs have entered clinical trials for tumor therapy [4].
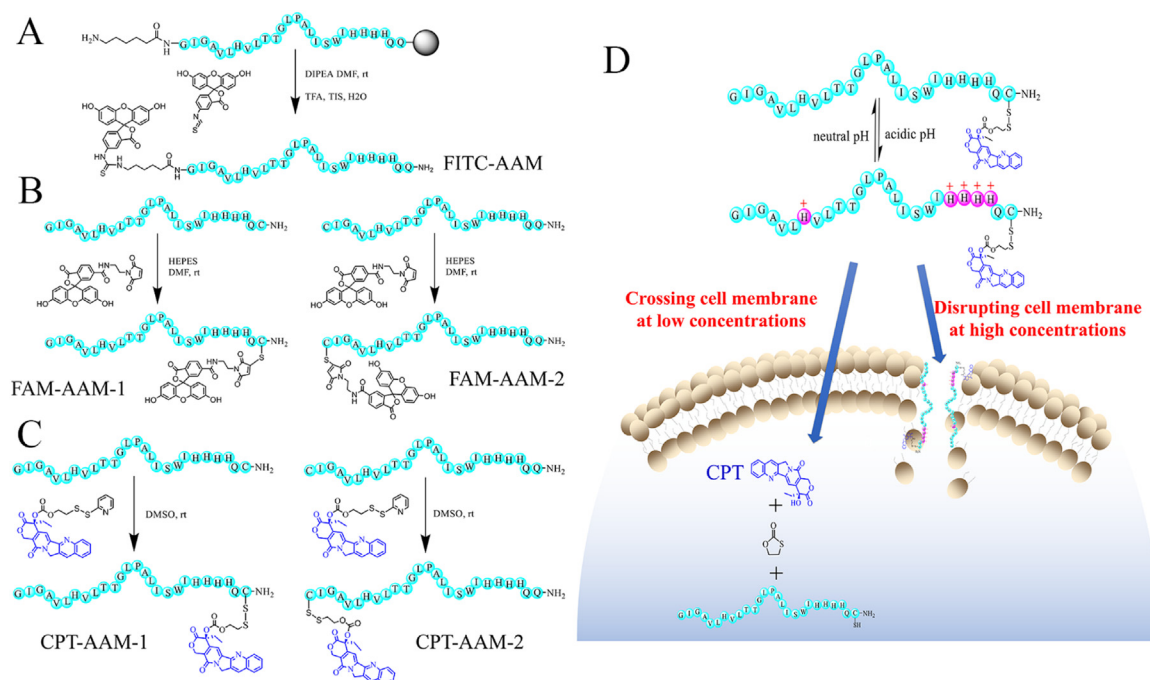
Melittin, which is derived from bee venom, is a classical AMP with multiple functions [5,6]. In recent years, melittin has

---

Scheme 1 – Synthesis of (A) FITC-AAM, (B) FAM-AAM-1 and FAM-AAM-2, and (C) CPT-AAM-1 and CPT-AAM-2. (D) Schematic illustration of antitumor mechanism of CPT-AAM-1.

been widely used for tumor treatment because of its robust membrane-lytic activity [5,7,8]. In addition, melittin has been found to penetrate cell membrane without damaging it at low concentrations, similar to cell-penetrating peptides (CPPs) [9–11]. Therefore, melittin can be used as an efficient vector to deliver various types of cargo into cells. In our previous study, stearylated melittin and its retro isomer were able to deliver p53 plasmid DNA into cells [12]. Although melittin has shown widespread use, its extreme toxicity and limited specificity greatly hamper its clinical application in tumor therapy.

Recently, several strategies that exploit the tumor microenvironment (such as acidic pH and matrix metalloprotease enzymes) have been investigated to improve the tumor specificity of AMPs and CPPs [7,11,13-15]. The electrostatic attraction between cationic AMPs or CPPs and the anionic components of tumor cell membranes plays a pivotal role in membrane binding and subsequent membrane disruption or penetration [13,16-18]. The pH response strategy for controlling electrostatic interactions has been shown to be effective in improving the tumor specificity of AMPs and CPPs [11,13,15,19,20].

Histidine, which contains an imidazole side chain, is the only amino acid that can shift from the unprotonated state at neutral pH to the protonated state for a positive charge at mildly acidic pH. In this regard, histidine has been utilized to construct pH-responsive AMPs or CPPs with enhanced specificity for tumor cells [15,21-23]. Our previous studies have also shown that replacing lysines and arginines with histidines is an effective strategy for designing acid-activated CPPs [20,24,25]. In this study, we designed novel melittin analogs with strong pH-responsive, membrane-lytic, and cell-penetrating activities. To this end, we synthesized pH-responsive analogs by replacing the lysine

and arginine residues in melittin with histidine (Scheme 1 and Table S1). The antitumor drug camptothecin (CPT) was conjugated to the melittin analogs via a disulfide-releasing carbonate linker (Scheme 1C). We expected that these melittin analog-CPT conjugates would possess two functions under acidic conditions (Scheme 1D): at high concentrations, they would kill tumor cells by membrane disruption, and at low concentrations, they would kill tumor cells by releasing CPT. To the best of our knowledge, there are no reports on these types of histidine-containing melittin analogs or their corresponding antimicrobial peptide-drug conjugates. Therefore, a series of experiments was performed to examine the cell-penetrating, membrane-lytic, and antitumor activities of the developed melittin analogs and their conjugates.

2. Materials and methods

2.1. Materials

Hydroxybenzotriazole, O-benzotriazole-N,N,N',N'-tetramethyl-uronium-hexaf were purchased from GL Biochem Ltd (Shanghai, China). MBHA resin were purchased from Nangkaihecheng Ltd (Tianjin, China). N,N-diisopropylethylamine, trifluoroacetic acid, triisopropylsilane, 1,2-ethanedithiol and piperidine were purchased from Sigma-Aldrich (USA). FAM maleimide (6-isomer) and Cy5.5 maleimide were purchased from Lumiprobe (USA). CPT was purchased from Innochem (Beijing, China), 2,2-dithiodipyridine, 2-mercaptoethanol, 4-dimethylaminopyridine and triphosgene were purchased from Meryer (Shanghai, China). Acetonitrile was purchased from Energy Chemical (Shanghai, China). N,N-

dimethylformamide was purchased from Rongcheng Chemical (Chengdu, China). Methanol, dichloromethane, trichloromethane, ethyl acetate, petroleum ether and diethyl ether were purchased from Rionlon (Tianjin, China). DMEM medium and fetal bovine serum (FBS) were purchased from Gibco BRL (USA). Propidium iodide (PI), calcein, 3-(4,5-dimethyl-2-thiazolyl)−2,5-diphenyl tetrazolium bromide (MTT), Triton X-100, dimethyl sulfoxide and Cremophor EL were purchased from Sigma-Aldrich (USA). Propidium Iodide Kit was purchased from ThermoFisher Scientific (USA). CytoTox-ONE kit for LDH release assay was purchased from Promega (USA). LysoTracker Red was purchased from Beyotime Biotechnology (Shanghai, China).

2.2. Cells and animals

B16-F10 cells were cultured in DMEM medium supplemented with 10% FBS at 37 °C under 5% CO_2 humidified atmosphere. Six-week-old female C57BL/6 mice were provided by Lanzhou Veterinary Research Institute. Animal experiments were conducted in accordance with the European Community Guidelines. Animal studies were approved by the Ethics Committee and Institutional Animal Care and Use Committee of Lanzhou University (Permit Number: SYXK Gan 2018-0002).

2.3. Synthesis of peptides and peptide-CPT conjugates

All peptides were synthesized by standard Fmoc-based SPPS method. FITC-labeled peptides and peptide-CPT conjugates were synthesized as previously described [26]. The fluorescein moiety (FAM maleimide or Cy5.5 maleimide, 3 mg) was linked via a thioether bond to the cysteine residue of peptides (9 mg) in 2 ml HEPES buffer at room temperature for 12 h. All compounds were purified and analyzed by HPLC using a C_{18} column and then characterized by ESI-TOF. FITC-TP10, melittin, FITC-melittin, TH and D-H6L9 used in this study were previously synthesized in our lab.

2.4. Cellular uptake assay

To determine the cell-penetrating activity of melittin analogs, 1×10^5 B16-F10 cells were seeded in each well of a 24-well microplate and cultured overnight. After 1-h incubation with serum-free medium containing FITC-labeled (5 µM) or FAM-labeled peptides (5 µM) at different pH conditions, the cells were harvested and subsequently analyzed by BD FACS Caliber.

To visualize the internalization of melittin analogs and peptide-CPT conjugates, 6×10^4 B16-F10 cells were seeded in a glass-bottomed culture dish and cultured overnight. After 1-h treatment with serum-free medium containing FAM-labeled peptides (5 µM) or peptide-CPT conjugates (5 µM) at pH 7.4 or 5.5, the cells were washed with PBS and subsequently visualized by Zeiss LSM 710 confocal microscope.

2.5. Endosome escape assay

To visualize the effect of melittin analogs on endosomal membrane stability, 6×10^4 B16-F10 cells were seeded in a glass-bottomed culture dish and cultured overnight. After 1 h treatment with serum-free medium containing calcein (30 µg/ml) with or without peptides (5 µM) at pH 5.5, the medium was removed, and LysoTracker Red (100 nM) was added to stain lysosomes for another 30 min. Finally, the cells were washed with PBS and visualized by confocal microscope.

To visualize the endosomal escape of melittin analogs, 6×10^4 B16-F10 cells were seeded in glass-bottomed culture dish and cultured overnight. After 1-h treatment with serum-free medium containing FAM-labeled peptides (5 µM) at pH 5.5, the medium was removed and LysoTracker Red (100 nM) was added to stain lysosomes for another 30 min. Finally, the cells were washed with PBS and visualized by confocal microscope. To evaluate the endosomal escape ability of peptides at different incubation times, cells were treated with FAM-AAM-1 (5 µM) at pH 5.5 for 15 min (This time point was considered as 0 min). Following further incubation for 15, 30 and 60 min, the medium was removed and LysoTracker Red (100 nM) was added to stain lysosomes for another 30 min. The quantification of co-localization was performed by means of Pearson's correlation coefficient (R) utilizing the ImageJ software.

2.6. In vitro drug release

To estimate the drug release behavior of CPT-AAM-1 in different conditions, the CPT-AAM-1 solution was added to a solution containing 10 mM of glutathione (GSH) or 10 mM of dithiothreitol (DTT) at a final concentration of 1 mg/ml. Samples were analyzed using RP-HPLC at predominant time points (UV detection at 220 nm).

2.7. Circular dichroism (CD) measurements

AAM and peptide-CPT conjugates were dissolved in a 50% TFE/PBS (v/v) solution with pH 7.4 or 5.5 at a concentration of 50 µM. CD spectra of the peptides from 195 to 260 nm were obtained on a J1500 spectrophotometer, with a scanning speed of 50 nm/min, step size of 0.1 nm, and a duration of 0.5 s using a 2 mm path length cell.

2.8. In vitro cytotoxicity assay

To study the in vitro antitumor activity of free CPT and conjugates, 5×10^3 B16-F10 cells were seeded in each well of a 96-well plate and cultured overnight. After 1 h treatment with compounds at pH 5.5 or 7.4, the remaining supernatant was replaced with fresh serum-contained DMEM and cultured for another 72 h. The cytotoxicity of compounds was evaluated by MTT assay.

To study the short-term cytotoxicity of peptides and their conjugates, 1×10^4 B16-F10 cells were seeded in each well of a 96-well plate and cultured overnight. After 1 h incubation with compounds at different pH conditions. The cytotoxicity of compounds was evaluated by MTT assay. Melittin, D-H6L9 and TH were used as positive controls.

2.9. Caspase-3 activity assay

B16-F10 cells (5×10^5) were seeded in each well of a 6-well plate and cultured overnight. Following treatment with

peptides for 24 h, caspase-3 activity was assessed using a Caspase-3 assay kit (Beyotime).

2.10. Cell cycle assay

To evaluate the influence of melittin analogs and their conjugates on cell cycle, 2×10^5 B16-F10 cells were seeded in each well of a 6-well plate and cultured overnight. After 1 h treatment with melittin (2 µM), CPT (5 µM), AAM analogs (5 µM) and conjugates (5 µM) at pH 5.5, the remaining supernatant was replaced with fresh serum-containing DMEM and cultured for another 24 h. Subsequently, cells were collected and fixed in 70% ethanol overnight. After staining with PI according to the operation manual of the kit, the cell cycle was analyzed by flow cytometry.

2.11. LDH release assay

To study the effects of melittin analogs and their conjugates on the membrane integrity, 1×10^4 B16-F10 cells were seeded in each well of a 96-well plate and cultured overnight. After 1 h treatment with compounds at pH 7.4 or 5.5. The LDH release of cells was evaluated by CytoTox-ONE Kit (Promega). Untreated cells were defined as no LDH leakage and total LDH release from cells lysed with lysis solution was defined as 100% LDH leakage.

2.12. PI uptake assay

To study the membrane-disruptive activity of melittin analogs and their conjugates, 6×10^4 B16-F10 cells were seeded in glass-bottomed culture dish and cultured overnight. After 1 h treatment with different agents (10 µM) at pH 5.5, the remaining agents were replaced with fresh DMEM containing PI solution (1 µg/ml). After 10 min incubation, the cells were visualized by confocal microscope. The cells treated with melittin were used as positive controls.

To further study the membrane-lytic kinetics of melittin analogs and their conjugates, 6×10^4 B16-F10 cells were seeded in glass-bottomed culture dish and cultured overnight. After replacing the medium with DMEM containing PI (1 µg/ml) at pH 5.5, different agents were added to the solution at a final concentration of 10 µM. Immediately, the time-lapse imaging of cells was visualized by confocal microscope and images were taken every 1 min for 30 min.

2.13. Hemolysis assay

To study the hemolytic activity of melittin analogs and their conjugates, whole mouse blood was collected in heparin tubes. After a centrifuge (1,000× g) for 15 min, the pellets were washed three times with PBS and resuspended in PBS to 10% (v/v). The erythrocyte suspension was mixed with different compounds in 96-well plate for 1 h at 37 °C. After centrifuge, the supernatants (100 µl) were collected and the absorbance at 450 nm was detected. Cells treated with PBS and 0.1% Triton X-100 were used for 0 and 100% hemolysis, respectively.

2.14. In vivo antitumor efficacy study

To study the in vivo antitumor activity of AAM, AAM-1 and CPT-AAM-1, 5×10^5 B16-F10 cells were injected subcutaneously into the right flank of female C57BL/6 mice (8 mice/group). When the tumor volume reached 40–50 mm^3, 50 µl PBS (pH 5.5) containing CPT (0.02 mg), peptides (0.2 mg) or conjugates (0.2 mg) was intratumorally injected once a day for three consecutive days. The first day of injections was designated as Day 0. Tumor sizes and mouse weight were measured on Day 0, 1, 2, 3, 6, 9, 12 and 15. The subcutaneous tumor volume was calculated based on the following formula: volume = length × (width)^2 × 0.5. To evaluate the effects of therapy and the toxicity of compound, tumor tissue and major organs were excised on Day 3 and stained with hematoxylin and eosin (H&E) for histopathologic examination.

2.15. In vivo and ex vivo fluorescence imaging

When the tumor volume reached 70–100 mm^3, mice ($n = 4$) were treated with a single intratumoral injection of Cy5.5-AAM-1 at a dose of 0.2 mg. Whole-body optical images were taken at predominant time points (0, 1, 4 and 24 h) using fluorescence imaging system (VISQUE® Invivo Smart-LF). At 24 h after injection, the mice were sacrificed, and the tumor tissues and major organs were excised. After washing with PBS, the optical images of the tumor tissues and major organs were taken using fluorescence imaging system.

2.16. Statistical analysis

The experimental data obtained from three independent experiments were expressed as means ± SD. Statistical analysis was made using one-way ANOVA. $P < 0.05$ was considered to indicate a significant difference.

3. Results and discussion

3.1. pH-responsive cellular uptake of histidine-containing melittin analogs

First, FITC-labeled melittin and histidine-containing AAM were synthesized by conjugating the classical fluorescent molecule FITC to their N-terminal amino groups (Scheme 1A). Based on our previous experience, the antimicrobial peptide melittin, which has extremely strong membrane-lytic activity, displays high cell-penetrating activity at low concentrations [27,28]. However, the results derived from flow cytometry showed that FITC-melittin displayed lower cellular uptake than the positive control FITC-TP10 (Fig. 1A), which is a classical CPP with high cell-penetrating activity [29]. In addition, FITC-AAM at pH 5.5 showed approximately two-fold high cell-penetrating activity compared with pH 7.4 (Fig. 1A and S1A). Overall, the cell-penetrating activity of FITC-AAM did not reach the desired level. We postulated that conjugation of the FITC molecule to the N-terminal amino groups of melittin and AAM might impair their cell-penetrating activity. In this context, we designed and synthesized AAM-1 with a
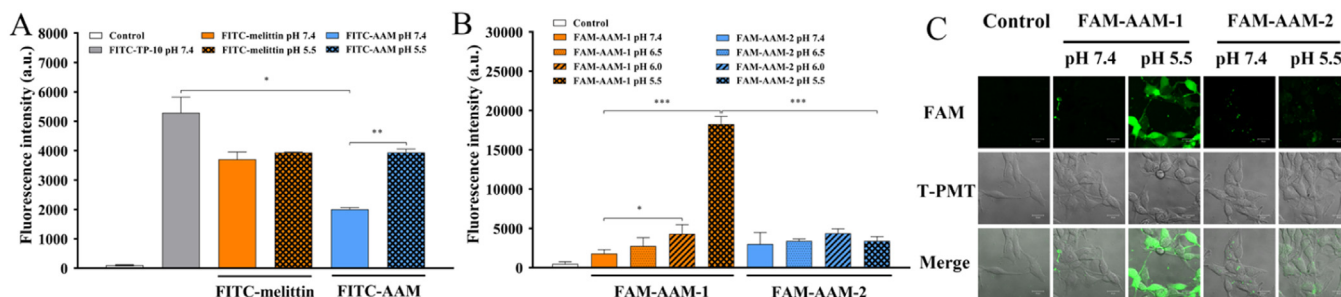
Fig. 1 – Cellular uptake of melittin and its analogs at different pH values. Flow cytometry analysis of B16-F10 cells treated with 5 μM of (A) FITC-labeled peptides or (B) FAM-labeled peptides after 1 h incubation. (C) Confocal images of B16-F10 cells treated with FAM-labeled peptides. Data represent the mean ± SD ($n = 3$). *$P < 0.05$, **$P < 0.01$, ***$P < 0.001$.

glutamine-to-cysteine substitution at position 26 of AAM and AAM-2 with a glycine-to-cysteine substitution at position 1 of AAM. Subsequently, 6-FAM maleimide was conjugated to the thiols of the cysteine residues of AAM-1 and AAM-2 by a stable thioether bridge (Scheme 1B). Fig. 1B and S1B show that the cellular uptake of FAM-AAM-1 displayed a significant pH-dependent effect, whereas FAM-AAM-2 displayed no obvious increase in cell-penetrating activity under acidic conditions compared to that at pH 7.4. Notably, FAM-AAM-1 at pH 5.5 showed approximately ten-fold high cell-penetrating activity compared with pH 7.4, indicating that FAM-AAM-1 displayed strong cell-penetrating activity under acidic conditions. In addition, FAM-AAM-1 displayed significantly stronger cell-penetrating activity than FAM-AAM-2 at pH 5.5. Confocal microscopy results showed that FAM-AAM-1 exhibited higher cellular uptake in B16-F10 cells at pH 5.5 than that at pH 7.4, whereas FAM-AAM-2 weakly exhibited this tendency (Fig. 1C). This result strongly supported the flow cytometry data, implying that AAM-1 derived from the antimicrobial peptide melittin has strong cell-penetrating activity. In addition, our results demonstrate that the C-terminus of AAM is more suitable for drug conjugation than its N-terminus.

In addition to direct translocation through the plasma membrane, endocytosis-mediated uptake has been demonstrated to be the major route for the cellular uptake of most CPPs [30,31]. Therefore, many modification strategies have been employed to promote endosomal escape of CPPs, such as the introduction of histidine or conjugation with membrane-lytic peptides [32–36]. To evaluate the effects of AAM-1 and AAM-2 on endosomal membrane integrity, a calcein leakage assay was performed. Calcein can be used as a probe to evaluate endosomal membrane disruption because its fluorescence becomes bright green after escaping the endosome into the cytoplasm [20,35]. Fig. 2A showed that untreated cells displayed yellow fluorescence, indicating that calcein was entrapped in the endosomes. Green fluorescence in AAM-1-treated cells became brighter, whereas an increase in green fluorescence in AAM-2-treated cells was not apparent. This result demonstrates that AAM-1 displays stronger endosome-disruption activity than AAM-2. To evaluate the endosomal escape activity of these analogs, we observed the co-localization between FAM-labeled analogs and LysoTracker Red-labeled endosomes. As shown in Fig. 2B, most of the green fluorescence was seen in B16-F10 cells

after treating with FAM-AAM-1 at pH 5.5, whereas relatively little yellow fluorescence (overlap of the green fluorescence of FAM-labeled analogs and the red fluorescence of LysoTracker Red-labeled endosomes/lysosomes) was visible. This result demonstrates that a large number of FAM-AAM-1 molecules were in the cytoplasm rather than in the endosome, indicating the high endosomal escape activity of AAM-1. In contrast, more yellow fluorescence was seen in FAM-AAM-2-treated cells, indicating that AAM-2 has weaker endosomal escape activity than AAM-1. In addition, we further explored the endosomal escape of FAM-AAM-1 at different incubation times. Fig. 2C showed that the yellow fluorescence intensity in B16-F10 cells after FAM-AAM-1 treatment became gradually weak with prolonged incubation time. In addition, we quantified the endosomal localization of FAM-AAM-1 by calculating the Pearson's correlation coefficients (r) between the green fluorescence signals from FAM-AAM-1 and the red fluorescence signals from LysoTracker Red. Fig. 2D showed that the r-values became gradually low over time, indicating that more FAM-AAM-1 molecules escaped from the endosome. In short, high endosomal escape efficiency implies that AAM-1 may be capable of delivering more drugs into the cytoplasm to exert its functions.

3.2. Drug release of histidine-containing melittin analog-CPT conjugates

Peptide-drug conjugates (PDCs) represent an effective strategy for improving tumor specificity and overcoming efflux-mediated multidrug resistance to conventional chemotherapy drugs [37–39]. Owing to tumor heterogeneity, CPPs exhibit certain advantages for antitumor drug delivery compared with tumor cell surface receptor-targeting peptides [39,40]. Histidine-containing CPPs with acid-activated cell-penetrating activity are considered efficient carriers for selectively delivering conventional antitumor drugs into tumor cells [23,24,41]. Therefore, we synthesized acid-activated PDCs by attaching the antitumor drug, CPT, to AAM-1 and AAM-2 using a disulfide-releasing carbonate linker (Scheme 1C). The free thiol formed after reduction can cyclize into the proximate carbonyl group of the linker, resulting in the release of free CPT (Scheme 1D). To evaluate the release of CPT from conjugate, we established the sensitivity of CPT-AAM-1 to biochemical reduction. Our results showed
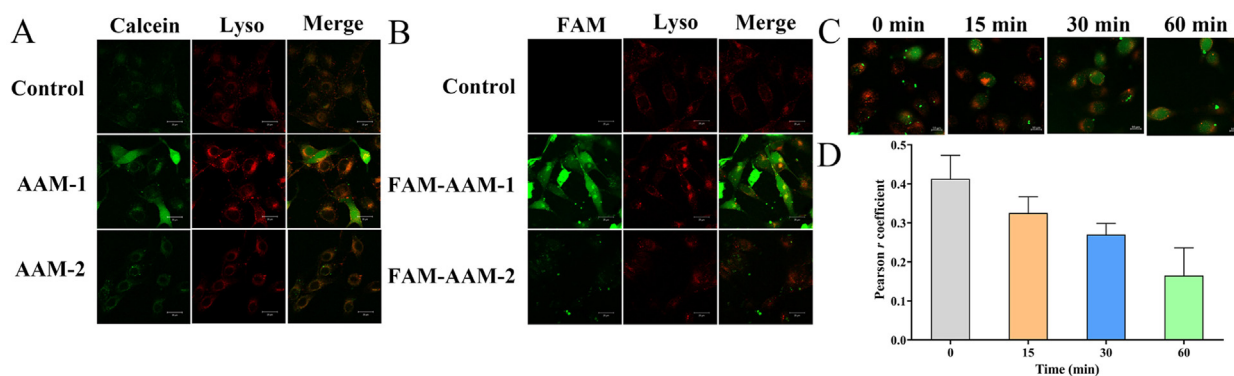
Fig. 2 – Endosomal escape of peptides: (A) Confocal images of B16-F10 cells co-treated with calcein and peptides (5 μM) for 1 h at pH 5.5. (B) Confocal images of endosomal/lysosomal localization of FAM-labeled peptides (5 μM) in B16-F10 cells. Cells were treated with 5 μM of FAM-labeled peptides for 1 h at pH 5.5. (C) Confocal images of endosomal/lysosomal localization of FAM-AAM-1 (5 μM) in B16-F10 cells at predominant time points. (D) Pearson correlation coefficients between FAM-AAM-1 and endosome/lysosome.
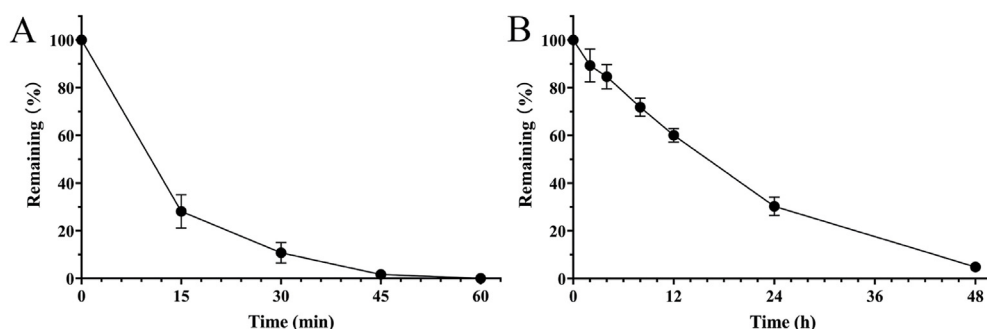

Fig. 3 – Stability of CPT-AAM-1 in (A) 10 mM of DTT solution and (B) 10 mM of GSH solution.

that the degradation of CPT-AAM-1 occurred in DTT or GSH solution, accompanying by the release of CPT (Fig. 3, S2 and S3). The degradation rate of CPT-AAM-1 in DTT solution was clearly faster than that in GSH solution, possibly owing to the weaker reducing power of GSH.

3.3. Structure of histidine-containing melittin analog-CPT conjugates

The α-helical structure has been identified as a critical factor in regulating the membrane-permeabilizing activity of melittin [42]. Consequently, we studied the second structures of AAM, CPT-AAM-1 and CPT-AAM-2 in a TFE/PBS solution with pH values of 7.4 or 5.5. As shown in Fig. S4, AAM, CPT-AAM-1 and CPT-AAM-2 exhibited typical α-helical structures, and their helical content did not show a significant difference. Maintaining a certain degree of helical conformation is an important condition for these conjugates to exert membrane-permeabilizing activity.

3.4. pH-responsive cytotoxicity of histidine-containing melittin analog-CPT conjugates

The cellular uptake of CPT-AAM-1 and CPT-AAM-2 was observed using confocal microscopy. As shown in Fig. 4A,

blue fluorescence under near UV excitation was observed in CPT-treated B16-F10 cells at different pH values, while the distinction of fluorescence intensity between pH 7.4 and pH 5.5 was not obvious. Contrastly, the fluorescence intensity in CPT-AAM-1- and CPT-AAM-2-treated cells at pH 5.5 was stronger than that at pH 7.4, demonstrating that the cellular uptake of CPT-AAM-1 and CPT-AAM-2 was pH-dependent. More importantly, the fluorescence intensity in CPT-AAM-1-treated cells was stronger than that in CPT- and CPT-AAM-2-treated cells at pH 5.5, implying that CPT-AAM-1 may display high antitumor activity under acidic conditions.

Subsequently, the cytotoxicity of these conjugates against B16-F10 cells was determined. As shown in Fig. 4B, CPT-AAM-1 and CPT-AAM-2 displayed significant pH-dependent antitumor activity after 72 h of treatment, whereas the cytotoxicity of CPT showed no obvious difference at pH 7.4 and 5.5. Notably, CPT-AAM-1 and CPT-AAM-2 exhibited greater cytotoxicity than free CPT under acidic conditions, particularly at high concentrations. Compared to CPT-AAM-2, CPT-AAM-1 displayed strong antitumor activity, suggesting that AAM-1 could deliver more CPT molecules into cells. In addition, this result further demonstrates that the C-terminus of AAM is more suitable for drug conjugation than the N-terminus.
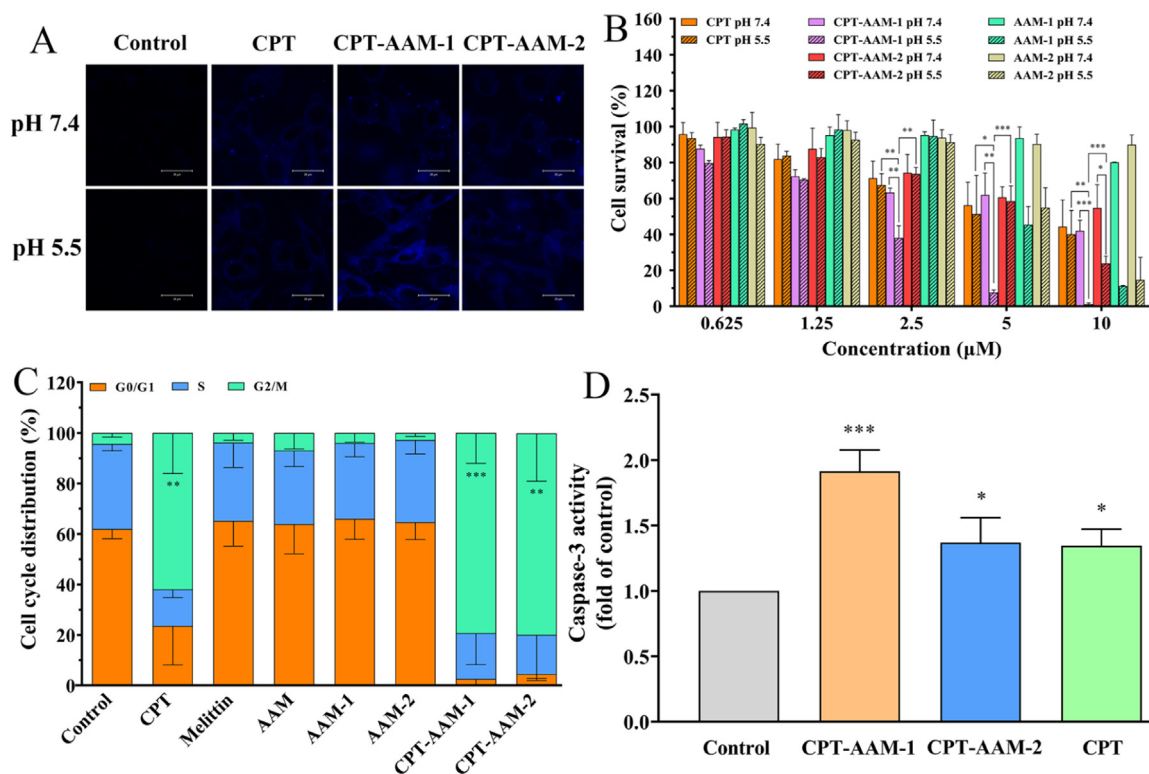
Fig. 4 – (A) Confocal images of B16-F10 cells treated with peptide-CPT conjugates (5 μM) for 1 h at different pH values. (B) Cytotoxicity of peptides and conjugates against B16-F10 cells after 72 h incubation. *P < 0.05, **P < 0.01, ***P < 0.001. (C) Cell cycle distribution of B16-F10 cells treated with different peptides and conjugates at pH 5.5 for 24-h incubation. Data represent the mean ± SD (n = 3). **P < 0.01, ***P < 0.001 versus control. (D) Determination of caspase-3 activation in conjugate-treated B16-F10 cells. *P < 0.01, ***P < 0.001 versus control.

To confirm the role of CPT in the cytotoxicity of CPT-AAM-1 and CPT-AAM-2, the cell cycle alternation was detected after 24 h of drug treatment. As shown in Fig. 4C and S5, CPT significantly increased the cell proportion in the G2/M phase and decreased the cell proportion in the G0/G1 and S phases, whereas AAM-1- and AAM-2-treated cells showed no obvious changes in the cell cycle. In contrast, CPT-AAM-1 and CPT-AAM-2 induced a higher cell proportion in the G2/M phase than CPT alone. As an inducer of apoptosis, CPT can initiate the intrinsic pathway by activating caspase-3 [43]. Consequently, the activation of caspase-3 in CPT-AAM-1- and CPT-AAM-2-treated cells was detected using a caspase activity assay kit. As shown in Fig. 4D, CPT, CPT-AAM-1 and CPT-AAM-2 significantly activated caspase-3, and CPT-AAM-1 caused more caspase-3 activation. These results demonstrate that CPT-AAM-1 and CPT-AAM-2 inhibited cell growth by releasing CPT upon entry into cells.

3.5. pH-responsive membrane-lytic activity of histidine-containing melittin analog-CPT conjugates

The typical mechanism of action of AMPs is membrane disruption, which not only effectively kills conventional drug-resistant tumor cells, but also does not easily induce drug resistance [4,16]. More importantly, AMPs can target tumor heterogeneity by driving antitumor immune responses induced by the release of danger-associated molecular patterns (DAMPs) from membrane-damaged cells [4]. Based on the strong membrane-lytic activity of melittin, we expected that histidine-containing melittin analogs and their conjugates would kill tumor cells by membrane disruption in a pH-dependent manner.

To understand the short-term cytotoxicity of melittin analogs and their conjugates, the MTT assay was used to evaluate their cytotoxicity against B16-F10 cells at various pH values after 1 h of incubation. Fig. S6 showed that melittin exhibited high cytotoxicity to B16-F10 cells, even at 1.25 μM, at various pH values, while its cytotoxicity displayed no obvious pH dependence. In contrast, the cytotoxicity of AAM was concentration- and pH-dependent. TH, a histidine-containing CPP developed in our laboratory, displays pH-responsive membrane-lytic activity at high concentrations [24]. D-H6L9, a histidine-containing AMP developed by Shai et al., displays pH-dependent antitumor activity [15]. Therefore, we selected TH and D-H6L9 as positive controls in this study. Although our results showed that AAM exhibited less cytotoxicity than melittin, its cytotoxicity was significantly stronger than that of TH and D-H6L9 especially at pH 6.0 and 5.5 (Fig. S6). Subsequently, the cytotoxicity of AAM-1, AAM-2, and their CPT conjugates at different pH values was evaluated after 1 h of drug treatment. AAM-1 showed similar levels of cytotoxicity against B16-F10 cells, whereas AAM-2
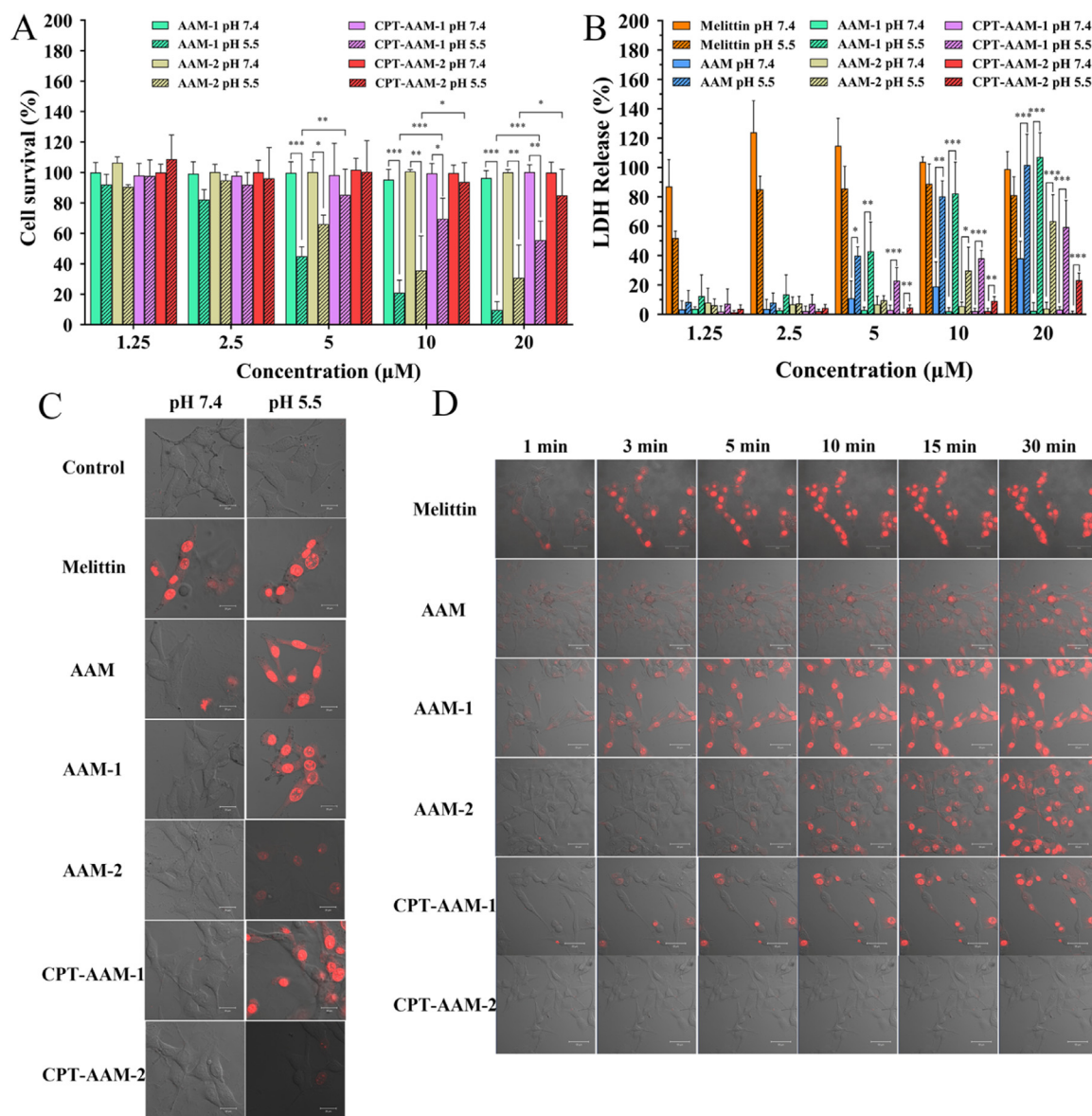
Fig. 5 – Membrane-lytic activity of peptides and peptide-CPT conjugates against B16-F10 cells at different pH values: (A) Short-term cytotoxicity of peptides and conjugates after 1 h incubation. (B) LDH release of cells treated with peptides and conjugates for 1 h. (C) PI uptake in B16-F10 cells treated with 10 μM of peptides and conjugates for 1 h. (D) Time-lapse images of B16-F10 cells treated with 10 μM of peptides and conjugates at pH 5.5 during 30 min. Data represent the mean ± SD ($n = 3$). *$P < 0.05$, **$P < 0.01$, ***$P < 0.001$.

showed an obvious decrease in cytotoxicity when compared with AAM (Fig. 5A and S6D). This result demonstrates that cysteine substitution at the N-terminus of AAM significantly decreased its cytotoxicity compared to substitution at the C-terminus. However, CPT conjugation decreased the cytotoxicity of CPT-AAM-1 and CPT-AAM-2 under acidic conditions (Fig. 5A). Despite this, CPT-AAM-1 and CPT-AAM-2 were still capable of killing tumor cells in a short period under acidic conditions. Compared with CPT-AAM-2, CPT-AAM-1 displayed higher cytotoxicity against B16-F10 cells. The short-term cytotoxicity of the melittin analogs and their conjugates suggests that they may kill cells via membrane disruption.

To evaluate the membrane-lytic activity of the melittin analogs and their conjugates, an LDH leakage assay was we performed. Fig. 5B showed that melittin induced a strong release of LDH at both pH 7.4 and 5.5 after 1 h of drug treatment, indicating that melittin had no obvious pH-responsive membrane-lytic activity. In contrast, all the histidine-containing analogs, including AAM, AAM-1, AAM-2, CPT-AAM-1 and CPT-AAM-2, induced LDH release in an obvious pH-dependent manner. This result strongly supported the result indicated by the MTT assay, suggesting that all tested analogs were capable of rapidly disrupting tumor cell membranes under acidic conditions. Compared with AAM-2, AAM and AAM-1 showed higher membrane-

lytic activity. In addition, CPT conjugation decreased the membrane-disruptive activity of CPT-AAM-1 and CPT-AAM-2. Despite this, CPT-AAM-1 showed higher membrane-disruptive activity than CPT-AAM-2.

To further confirm the membrane-disruptive activity of all analogs, PI uptake in cells was observed using CLSM. PI can be used to study the cell membrane integrity because it is a probe impermeable to membrane. As shown in Fig. 5C, the percentage of PI-positive B16-F10 cells after melittin treatment at pH 7.4 and 5.5 showed no obvious difference. Although the percentage of PI-positive cells after AAM treatment was increased at pH 5.5, a certain number of PI-positive cells at pH 7.4 was observed. This data was consistent with the results of the MTT and LDH leakage assays, indicating that AAM still displayed some degree of membrane-lytic activity at pH 7.4. In addition, PI uptake by B16-F10 cells after treating with AAM-1, AAM-2, CPT-AAM-1, and CPT-AAM-2 at pH 5.5 was obviously increased compared to that at pH 7.4, demonstrating that their membrane-disruptive activity was pH dependent. Notably, the membrane-disruptive activity of CPT-AAM-2 at pH 5.5 was obviously weaker than that of CPT-AAM-1, which was in agreement with the results of the MTT and LDH leakage assays. In addition, time-lapse images were acquired to observe the membrane-lytic behaviors of melittin, AAM, AAM-1, AAM-2, CPT-AAM-1, and CPT-AAM-2. As shown in Fig. 5D and Videos 1–6, after treatment with melittin, AAM, AAM-1, AAM-2 or CPT-AAM-1, B16-F10 cells developed necrosis, including rounding, blebbing, swelling, and bursting. Following the membrane disruption, PI rapidly entered the cells.

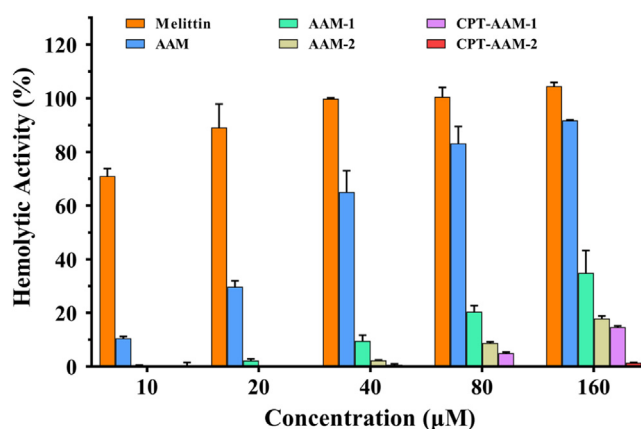Overall, the above results showed that these histidine-containing analogs could rapidly disrupt cell membranes

Fig. 6 – Hemolytic activity of peptides and peptide-CPT conjugates.

under acidic conditions. Notably, AAM-2 and CPT-AAM-2 with structural changes at the N-terminus displayed considerably weaker membrane-lytic activity than AAM-1 and CPT-AAM-1 with structural changes at the C-terminus. This demonstrates that the C-termini of the analogs are more suitable for structural modification and drug conjugation. In our previous studies, we confirmed that greater membrane disturbances yield higher cellular uptake of CPPs [27,28]. Therefore, the above results demonstrated that AAM-1, with stronger membrane-lytic activity, had higher cell-penetrating activity than AAM-2 (Fig. 1). In addition, many membrane-lytic peptides have been reported to facilitate endosomal escape of vectors by damaging the integrity of endosomal
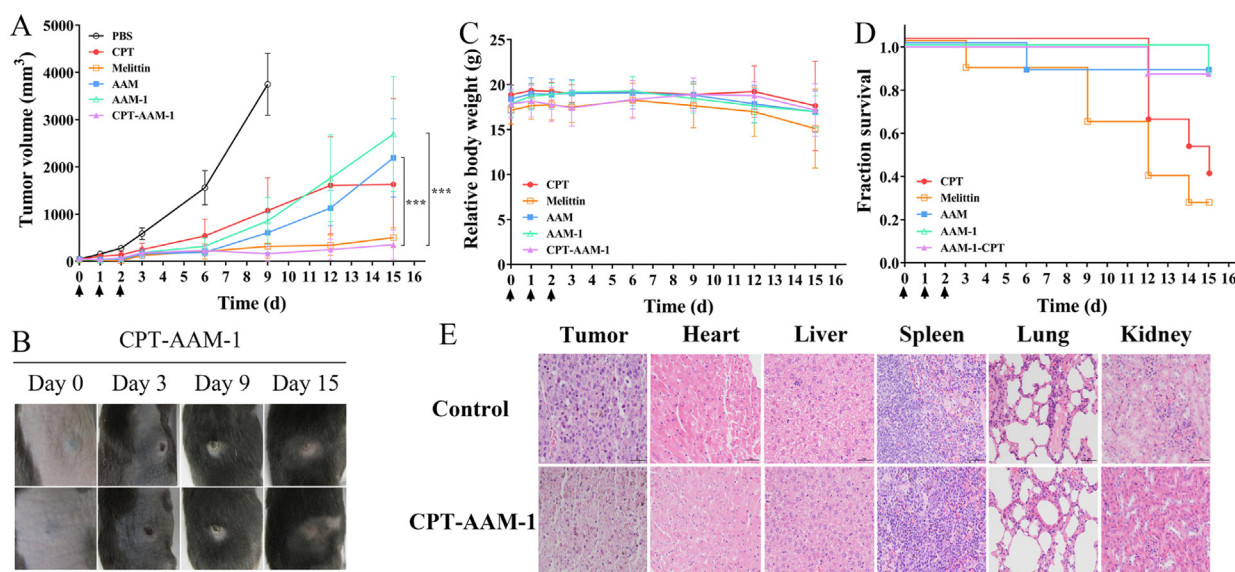

Fig. 7 – Antitumor activity of peptides and CPT-AAM-1 in a murine melanoma (B16-F10) model: (A) Tumor volume growth curves of tumors after intratumoral administration of peptides and CPT-AAM-1 once a day for 3 d consecutivly. The drug administration period and frequency were indicated with arrows. Data represent the mean ± SD ($n = 8$). *$P < 0.05$, ***$P < 0.001$ versus control. (B) Images of tumors in mice treated with CPT-AAM-1. (C) Body weight changes of mice treated with peptides and CPT-AAM-1. (D) Survival rates of tumor-bearing mice treated with peptides and CPT-AAM-1. (E) H&E staining of tumors and major organs on Day 3.
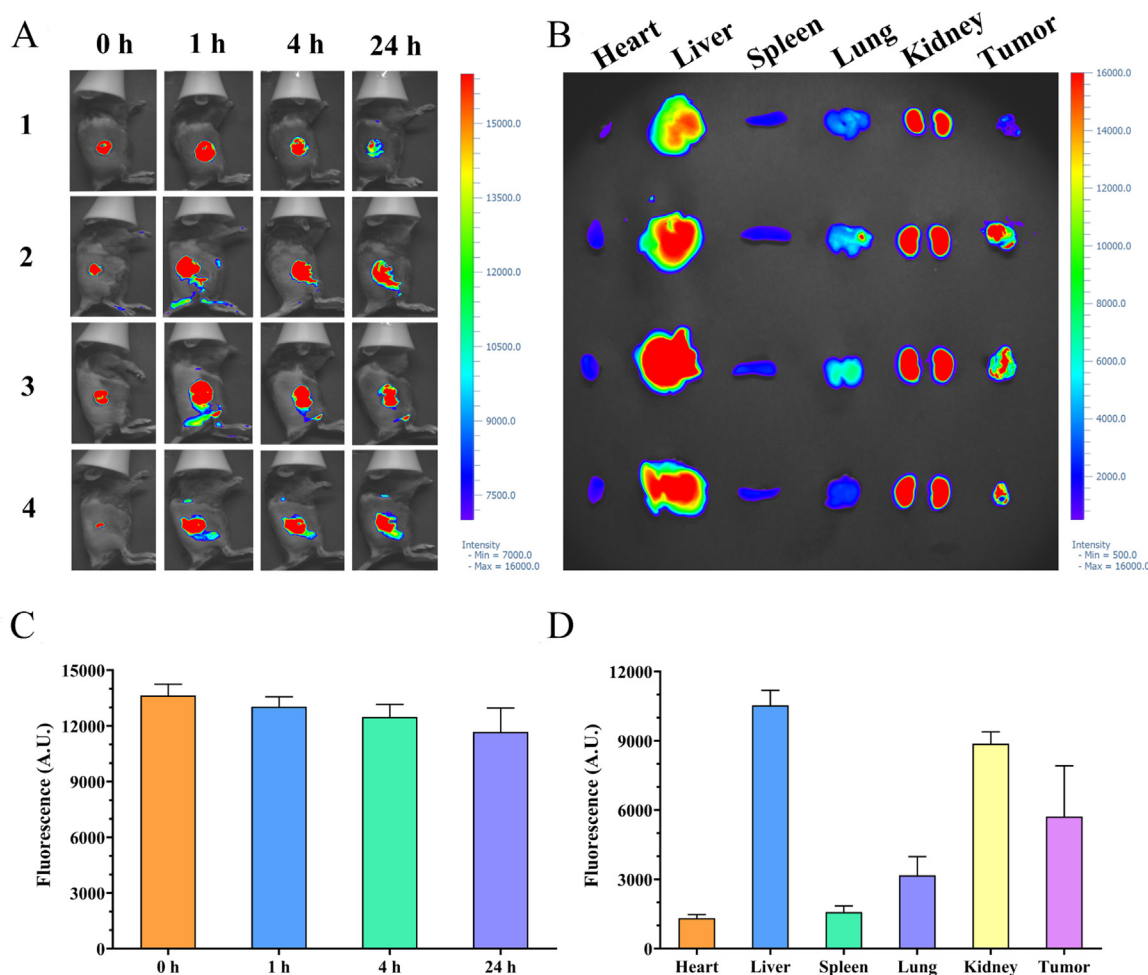
Fig. 8 – (A) *In vivo* **bioimaging behavior of B16-F10 tumor-bearing mice after intratumoral administration of Cy5.5-AAM-1. (B)** *Ex vivo* **bioimaging behavior of fluorescence images of the organs and tumor at 24 h after administration. (C) Quantification of fluorescence intensities in Fig. 8A. (D) Quantification of fluorescence intensities in Fig. 8B.**

membranes [35,44]. Our findings also demonstrated that AAM-1, with strong membrane-lytic activity under acidic conditions, displayed higher endosomal escape activity than AAM-2 (Fig. 2).

3.6. Hemolytic activity of histidine-containing melittin analog-CPT conjugates

Hemolysis assays are commonly used to determine AMP cytotoxicity against normal cells. In this study, melittin exhibited extreme hemolytic activity (Fig. 6). Although histidine substitution decreased the hemolytic activity of AAM compared to that of melittin, AAM did not lose its hemolytic activity as expected. Interestingly, the introduction of cysteine significantly decreased the hemolytic activity of AAM-1 and AAM-2. Additionally, the introduction of CPT further decreased the hemolytic activities of CPT-AAM-1 and CPT-AAM-2. Notably, introduction of cysteine or CPT at the N-terminus of AAM impaired its hemolytic activity compared to its C-terminus introduction. Overall, relatively low hemolytic activity makes these conjugates promising agents with low toxicity.

3.7. In vivo antitumor activity of histidine-containing melittin analog-CPT conjugates

Based on the above results, the in vivo antitumor efficacy of AAM, AAM-1, CPT-AAM-1, melittin, and CPT was evaluated in a B16-F10 murine melanoma model. As shown in Fig. 7A, all tested agents could obviously suppress melanoma tumor growth in mice. Compared with AAM and AAM-1, the *in vivo* tumor-suppressive activity of CPT did not increase. As expected, CPT-AAM-1 displayed significantly stronger in vivo tumor-suppressive activity than CPT or AAM-1 at the same dose (Fig. 7A). The H&E-stained tumor tissue sections revealed that CPT-AAM-1 treatment induced an extensive necrosis in comparison to the PBS treatment (Fig. 7E). Further, in two out of eight mice that received CPT-AAM-1 treatment, scabs formed at the tumor inoculation sites on Day 3 and almost completely disappeared on Day 15 (Fig. 7B). These two mice showed no tumor recurrence until Day 60. Although the *in vivo* tumor-suppressive activity of melittin was significantly higher than those of AAM and AAM-1, melittin induced higher mortality than AAM and AAM-1 (Fig. 7D). Compared with CPT treatment, CPT-AAM-1 treatment obviously extend

the survival of tumor-bearing mice (Fig. 7D). In addition, histopathological examination using H&E staining for major organs (heart, liver, spleen, lungs, kidney) in the CPT-AAM-1-treated groups showed no obvious tissue damage on Day 3 (Fig. 7E). Taken together, the above results demonstrate that CPT-AAM-1 exhibits potent antitumor efficacy with low toxicity *in vivo*.

To investigate the tissue biodistribution, Cy5.5-labeled AAM-1 was administered via a single intratumoral injection. The fluorescence images of mice were taken at predominant time points (0, 1, 4 and 24 h). Fig. 8A showed that the fluorescence signals were concentrated within the tumor sites at 0 h. Over time, the fluorescence was observed to gradually diffuse, accompanied by a slight reduction in fluorescence intensity (Fig. 8A and C). At 24 h after injection, the tumor tissues and major organs were excised for *ex vivo* fluorescence imaging. Fig. 8B and 8D showed that a high fluorescence intensity was seen in livers and kidneys, indicating the diffusion of a certain number of Cy5.5-labeled AAM-1 molecules into the bloodstream from the tumors. The fluorescence intensity of tumors *ex vivo* exhibited a significant reduction compared to that observed *in vivo*, indicating the occurrence of Cy5.5-labeled AAM-1 leakage from tumor tissues. Nonetheless, our results indicated that a certain number of CPT-AAM-1 remained in the tumor tissues to exert antitumor activity after 24 h of injection.

4.   Conclusions

In this study, we developed novel melittin analogs with pH-responsive cell-penetrating and membrane-lytic activities by replacing arginines and lysines with histidines. Importantly, we found that the conjugation of cargoes to the N-terminus of melittin analogs decreased their cell-penetrating and membrane-lytic activity compared to the C-terminus, implying that the C-terminus of analogs is more suitable for cargo conjugation. After the attachment of CPT, CPT-AAM-1 and CPT-AAM-2 displayed obvious pH-responsive antitumor activity. CPT-AAM-1 and CPT-AAM-2 destroyed tumor cells through the release of CPT and membrane disruption. Compared with CPT-AAM-2, CPT-AAM-1 showed stronger antitumor activity under acidic conditions. Notably, CPT-AAM-1 significantly inhibited the tumor growth *in vivo* compared with AAM, AAM-1, and CPT. In addition, CPT-AAM-1 showed relatively low toxicity compared with melittin and CPT. Taken together, our results demonstrate that CPT-AAM-1, with efficient pH-responsive cell-penetrating and membrane-lytic activities, possesses significant therapeutic potential for tumor therapy. This study provides a novel strategy for the development of PDCs based on pH-responsive AMPs for oncology therapeutics.

Conflicts of interest

The authors report no conflicts of interest. The authors alone are responsible for the content and writing of this article.

Acknowledgments

Supplementary materials

Supplementary material associated with this article can be found, in the online version, at doi:10.1016/j.ajps.2024.100890.

REFERENCES

[1] Singh M, Overwijk WW. Intratumoral immunotherapy for melanoma. Cancer Immunol Immunother 2015;64(7):911–21.

[2] Dharmadhikari N, Mehnert JM, Kaufman HL. Oncolytic virus immunotherapy for melanoma. Curr Treat Options Oncol 2015;16(3):326.

[3] Ylosmaki E, Cerullo V. Design and application of oncolytic viruses for cancer immunotherapy. Curr Opin Biotechnol 2020;65:25–36.

[4] Vitale I, Yamazaki T, Wennerberg E, Sveinbjornsson B, Rekdal O, Demaria S, et al. Targeting cancer heterogeneity with immune responses driven by oncolytic peptides. Trends Cancer 2021;7(6):557–72.

[5] Gajski G, Garaj-Vrhovac V. Melittin: a lytic peptide with anticancer properties. Environ Toxicol Pharmacol 2013;36(2):697–705.

[6] Guha S, Ferrie RP, Ghimire J, Ventura CR, Wu E, Sun LS, et al. Applications and evolution of melittin, the quintessential membrane active peptide. Biochem Pharmacol 2021;193:114769.

[7] Zhou J, Wan C, Cheng J, Huang H, Lovell JF, Jin HL. Delivery strategies for melittin-based cancer therapy. ACS Appl Mater Interfaces 2021;13(15):17158–73.

[8] Rady I, Siddiqui IA, Rady M, Mukhtar H. Melittin, a major peptide component of bee venom, and its conjugates in cancer therapy. Cancer Lett 2017;402:16–31.

[9] Kohno M, Horibe T, Ohara K, Ito S, Kawakami K. The membrane-lytic peptides K8L9 and melittin enter cancer cells via receptor endocytosis following subcytotoxic exposure. Chem Biol 2014;21(11):1522–32.

[10] Kiss E, Gyulai G, Pari E, Horvati K, Bosze S. Membrane affinity and fluorescent labelling: comparative study of monolayer interaction, cellular uptake and cytotoxicity profile of carboxyfluorescein-conjugated cationic peptides. Amino Acids 2018;50(11):1557–71.

[11] Luo L, Wu W, Sun D, Dai HB, Wang Y, Zhong Y, et al. Acid-activated melittin for targeted and safe antitumor therapy. Bioconjug Chem 2018;29(9):2936–44.

[12] Zhang W, Song J, Liang R, Zheng X, Chen J, Li G, et al. Stearylated antimicrobial peptide melittin and its retro isomer for efficient gene transfection. Bioconjug Chem 2013;24(11):1805–12.

[13] de Jong H, Bonger KM, Lowik D. Activatable cell-penetrating peptides: 15 years of research. RSC Chem Biol 2020;1(4):192–203.

[14] Raucher D, Ryu JS. Cell-penetrating peptides: strategies for anticancer treatment. Trends Mol Med 2015;21(9):560–70.

[15] Makovitzki A, Fink A, Shai Y. Suppression of human solid tumor growth in mice by intratumor and systemic inoculation of histidine-rich and pH-dependent host defense-like lytic peptides. Cancer Res 2009;69(8):3458–63.

[16] Baxter AA, Lay FT, Poon IKH, Kvansakul M, Hulett MD. Tumor cell membrane-targeting cationic antimicrobial peptides: novel insights into mechanisms of action and therapeutic prospects. Cell Mol Life Sci 2017;74(20):3809–25.

[17] Wakabayashi N, Yano Y, Kawano K, Matsuzaki K. A pH-dependent charge reversal peptide for cancer targeting. Eur Biophys J 2017;46(2):121–7.

[18] Khan MM, Filipczak N, Torchilin VP. Cell penetrating peptides: a versatile vector for co-delivery of drug and genes in cancer. J Control Release 2021;330:1220–8.

[19] Song J, Zhang W, Kai M, Chen J, Liang R, Zheng X, et al. Design of an acid-activated antimicrobial peptide for tumor therapy. Mol Pharm 2013;10(8):2934–41.

[20] Huang S, Zhu Z, Jia B, Zhang W, Song J. Design of acid-activated cell-penetrating peptides with nuclear localization capacity for anticancer drug delivery. J Pept Sci 2021;27(10):e3354.

[21] Chang LL, Bao HX, Yao J, Liu H, Gou SH, Zhong C, et al. New designed pH-responsive histidine-rich peptides with antitumor activity. J Drug Target 2021;29(6):651–9.

[22] Regberg J, Vasconcelos L, Madani F, Langel U, Hallbrink M. pH-responsive PepFect cell-penetrating peptides. Int J Pharm 2016;501(1–2):32–8.

[23] Nam SH, Jang J, Cheon DH, Chong SE, Ahn JH, Hyun S, et al. pH-Activatable cell penetrating peptide dimers for potent delivery of anticancer drug to triple-negative breast cancer. J Control Release 2021;330:898–906.

[24] Zhang W, Song J, Zhang B, Liu L, Wang K, Wang R. Design of acid-activated cell penetrating peptide for delivery of active molecules into cancer cells. Bioconjug Chem 2011;22(7):1410–15.

[25] Ji K, Xiao Y, Zhang W. Acid-activated nonviral peptide vector for gene delivery. J Pept Sci 2020;26(1):e3230.

[26] Henne WA, Doorneweerd DD, Hilgenbrink AR, Kularatne SA, Low PS. Synthesis and activity of a folate peptide camptothecin prodrug. Bioorg Med Chem Lett 2006;16(20):5350–5.

[27] Song JJ, Kai M, Zhang W, Zhang JD, Liu LW, Zhang BZ, et al. Cellular uptake of transportan 10 and its analogs in live cells: selectivity and structure-activity relationship studies. Peptides 2011;32(9):1934–41.

[28] Song JJ, Zhang Y, Zhang W, Chen JB, Yang XL, Ma PP, et al. Cell penetrating peptide TAT can kill cancer cells via membrane disruption after attachment of camptothecin. Peptides 2015;63:143–9.

[29] Soomets U, Lindgren M, Gallet X, Hallbrink M, Elmquist A, Balaspiri L, et al. Deletion analogues of transportan. Biochim Biophys Acta 2000;1467(1):165–76.

[30] Ramsey JD, Flynn NH. Cell-penetrating peptides transport therapeutics into cells. Pharmacol Ther 2015;154:78–86.

[31] Guidotti G, Brambilla L, Rossi D. Cell-penetrating peptides: from basic research to clinics. Trends Pharmacol Sci 2017;38(4):406–24.

[32] Hou KK, Pan H, Schlesinger PH, Wickline SA. A role for peptides in overcoming endosomal entrapment in siRNA delivery - a focus on melittin. Biotechnol Adv 2015;33(6):931–40.

[33] Lo SL, Wang S. An endosomolytic Tat peptide produced by incorporation of histidine and cysteine residues as a nonviral vector for DNA transfection. Biomaterials 2008;29(15):2408–14.

[34] Neundorf I, Rennert R, Hoyer J, Schramm F, Lobner K, Kitanovic I, et al. Fusion of a short HA2-derived peptide sequence to cell-penetrating peptides improves cytosolic uptake, but enhances cytotoxic activity. Pharmaceuticals 2009;2(2):49–65.

[35] Salomone F, Cardarelli F, Di Luca M, Boccardi C, Nifosi R, Bardi G, et al. A novel chimeric cell-penetrating peptide with membrane-disruptive properties for efficient endosomal escape. J Control Release 2012;163(3):293–303.

[36] Morais CM, Cardoso AM, Aguiar L, Vale N, Nobrega C, Zuzarte M, et al. Lauroylated histidine-enriched S413-PV peptide as an efficient gene silencing mediator in cancer cells. Pharm Res 2020;37(10):188.

[37] Zhou JQ, Li YY, Huang WL, Shi W, Qian H. Source and exploration of the peptides used to construct peptide-drug conjugates. Eur J Med Chem 2021;224.

[38] Vargas JR, Stanzl EG, Teng NN, Wender PA. Cell-penetrating, guanidinium-rich molecular transporters for overcoming efflux-mediated multidrug resistance. Mol Pharm 2014;11(8):2553–65.

[39] Dissanayake S, Denny WA, Gamage S, Sarojini V. Recent developments in anticancer drug delivery using cell penetrating and tumor targeting peptides. J Control Release 2017;250:62–76.

[40] Denison TA, Bae YH. Tumor heterogeneity and its implication for drug delivery. J Control Release 2012;164(2):187–91.

[41] Jiang TY, Zhang ZH, Zhang YL, Lv HX, Zhou JP, Li CC, et al. Dual-functional liposomes based on pH-responsive cell-penetrating peptide and hyaluronic acid for tumor-targeted anticancer drug delivery. Biomaterials 2012;33(36):9246–58.

[42] Krauson AJ, Hall OM, Fuselier T, Starr CG, Kauffman WB, Wimley WC. Conformational fine-tuning of pore-forming peptide potency and selectivity. J Am Chem Soc 2015;137(51):16144–52.

[43] Stefanis L, Park DS, Friedman WJ, Greene LA. Caspase-dependent and -independent death of camptothecin-treated embryonic cortical neurons. J Neurosci 1999;19(15):6235–47.

[44] Nadal-Bufí F, Henriques ST. How to overcome endosomal entrapment of cell-penetrating peptides to release the therapeutic potential of peptides? Peptide Science 2020;112(6):e24168.